

A Pupil Size Measurement System for the Analysis of the Impact of Flicker on Human Being

Maria Gabriella Masi¹, Lorenzo Peretto¹, Roberto Tinarelli¹, Luigi Rovati²

¹*Dipartimento Ingegneria Elettrica, Alma Mater Studiorum – Università di Bologna
Viale del Risorgimento, 2 I-40136 Italy*

<mariagabrella.masi,lorenzo.peretto, roberto.tinarelli>@mail.ing.unibo.it

²*Dipartimento di Ingegneria dell'Informazione, Università di Modena and Reggio Emilia
Via Vignolese, 905 I-41100 Italy
rovati.luigi@unimore.it*

Abstract- The validation of any new model of the human response to flicker requires proper experimental data. Recently, studies have been carried out with the intent of achieving information relevant to the state of annoyance of a human being subjected to light flicker by analyzing the modification of the pupil size. Indeed, it is well known that pupil diameter changes according to the luminous flux variation. According to such a theory the authors developed a measurement system capable of tracing the pupil size variations in time under flicker conditions. This will result of help for further developing the above theory and confirming its correctness and robustness.

The presented measurement system will allow measuring the pupil diameter when subjected to flicker with given amplitude, frequency and colour. The technique and the relative system will be examined through the description of some tests executed to evaluate its performance. The good behaviour of the measurement system suggests its future employment for the analysis of flicker effects on human beings.

I. Introduction

The instrument for flicker measurement is described by the standard EN 61000-4-15 [1] which has been recently adopted also by the IEEE as IEEE Standard 1453 [2]. As well known, the standard flickermeter operating principle relies on the analysis of the supply voltage which is processed according to a suitable model of the lamp – human eye – brain chain. As for the lamp, an incandescent 60 W, 230 V, 50 Hz source is assumed. As far as the human eye – brain model is concerned, it is represented by the so-called flicker curve. Such a curve was determined several years ago by statistically analyzing the results of tests where people were subjected to flicker with different combinations of magnitude and frequency. The observers reported their perception: people could say whether the flicker was perceived or not and, if yes, if it caused annoyance.

The limitations of this standard approach to flicker evaluation are essentially two. First, the provided index of annoyance Pst [1] can be related to an actual tiredness of the human visual system only if such an incandescent lamp is used. Moreover, the implemented response to flicker is “subjective” given that it relies on the people answers about their feelings.

In the last 15 years, many scientific contributions, see e.g. [3-11], have tackled these issues. By way of example, the adoption of suitable “gain factor” [3] or the implementation of novel model of the eye brain response to flicker [8-11] have been suggested to overcome the strict dependence of the standard [1] on the kind of light source. In particular, the model proposed in [8] and modified in [9] has shown quite interesting results when applied to different light sources [10]. Such a model relies on the analysis of the physiological mechanism of pupillary light reflex, i.e. the way the pupil area size varies as a consequence of changes in the level of ambient illumination. However, it must be kept in mind that the only real data available to test any new model are those which the standard [1] is based on.

In this light of fact, this paper is aimed at presenting and characterizing a system for the pupil size measurement in human being subjected to flicker.

This contribution is organized as follows: section II reviews the mechanism of pupillary light reflex and the eye-brain model that is based on; section III presents the system proposed to both generate flicker and measure the related pupil size variation. Finally, Section IV describes the characterization procedure.

II. Pupillary light reflex-based model

Pupil size can vary for two main reasons: i) changes in the ambient illumination and ii) changes in the distance between the eye and the object to be focused. The response of the human visual system is usually referred to as *pupillary light reflex* in the former case and *pupillary accommodation reflex* in the latter one.

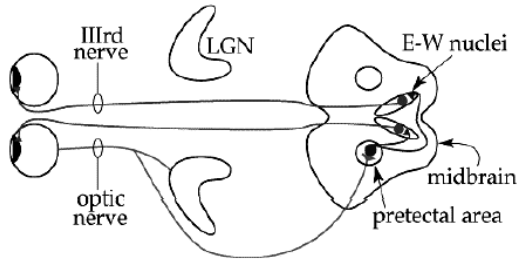


Fig. 1. Signal pathways in the pupillary light reflex

Let us briefly recall some basic physiological aspect. The light first enters the eye through the cornea and then through the pupil, which is a circular aperture in the iris. The crystalline lens converges the light rays into a focal point; namely the light progresses through the vitreous humour and it is focused on the central fovea and the macula which are the light-sensitive elements in the retina. In this tissue, a chemical reaction (photoreceptors) transforms the light impulse into electrical signals, which are then sent to the brain by the optic nerve. The region of the brain devoted to interpret such electrical signals is located in the occipital lobe: the signal bypasses the LGN (Lateral Geniculate Nucleus), which helps the visual system to focus its attention on the most important information, and arrives to pretectal nucleus that communicates with a suitable midbrain element (named Edinger-Westphal nuclei) aimed at managing the size of the pupillary aperture by driving the sympathetic and parasympathetic pathways. Such nerves, which are referred to as “3rd nerve” in Fig.1, control the movements of two opposing smooth muscles: the dilator and the sphincter (iris muscle). The flicker phenomena causes a continuous action of the dilator and the sphincter muscles, since the Edinger-Westphal (E-W) nuclei try to keep constant the amount of luminous intensity which reaches the central fovea and the macula. As a consequence, an annoyance sensation arises. This last effect must be ascribed to the energy spent for the iris muscles for forth and back motions. The signal pathways in the pupillary light reflex are also described in Fig. 1.

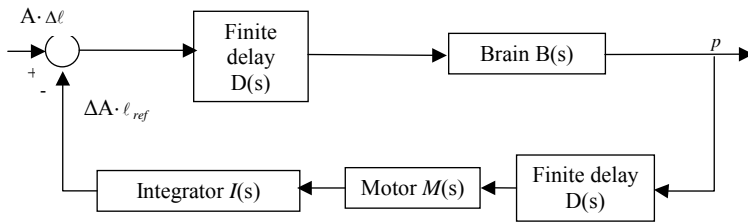


Fig. 2. Schematic block diagram of the pupillary light reflex - based model of the eye-brain system

On the basis of the above described physiological mechanism and under the assumption of small signals (i.e. small variations $\Delta\ell$ of luminance with respect to a bias value $\bar{\ell}$) the dynamic analytical model depicted in Fig. 2 has been derived in [8, 9]. In Fig. 2, A is the pupil area, the finite delay $D(s)$ models the behaviour of both the optic and IIIrd nerve, the motor $M(s)$ is used for describing the action of the iris muscles to vary the size of the pupil area, and finally the integrator $I(s)$ takes into account the mechanical inertia of the masses in motion. The output p is the instantaneous flicker sensation. The transfer function $H(s)$ of the network is:

$$H(s) = \frac{p(s)}{A(s) \cdot \Delta\ell} = \frac{p_2 s^2 + p_0}{q_8 s^8 + q_6 s^6 + q_4 s^4 + q_2 s^2 + q_0}, \quad (1)$$

where the parameters p_i and q_i take proper values [10].

III. The proposed system

The proposed system is shown in Fig. 3. It consists in two main blocks: i) the measurement section and ii) the generation section.

As for i), it is implemented by an high-speed high-resolution camera, a frame grabber and a personal computer. The camera (CM140MCL, Jai, Denmark), which is focused on an eye of the subject under test by means of an objective with a 50 mm focal length, is a digital monochrome progressive scan. It features 1380 x 1040 pixels, 31 frames-per-second (fps) at full resolution in continuous operation but

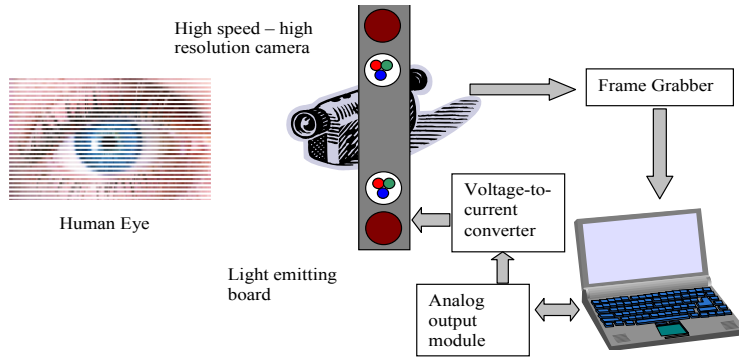


Fig.3 Schematic block diagram of the proposed system

can operate up to 62 fps if $\frac{1}{4}$ partial scan function is used. In such a case the pixel number decreases to 1380 x 269 but, of course, the resolution (expressed in pixel/mm) remains the same given that the camera reads a proportionally smaller centre portion of rows. CCD sensors has a spectral response ranging from 400 nm up to 1000 nm, thus allowing catching pictures

also in the near infrared region [12].

The frame grabber is made by National Instruments and, thanks to its camera link connection, allows real time storage of the camera output. The personal computer stores the acquired data and operates, through an ad-hoc software, developed by the authors under Labview environment, an off-line processing to get, frame by frame, the measure of the pupil diameter.

Essentially, it performs four steps: a) binarization of the image by using an automatically computed threshold; b) removal of particles having an area lower than 20% of the one of the whole image: this way reflected light spot are deleted; c) analysis of the previous region to get the pupil edge by applying the Sobel filter algorithm [14]; d) application of a weighted least square circular fitting [14] to obtain the pupil diameter.

As for the generation section ii), it consists in a light emitting diode board, a four channel voltage-to-current converter (one for each of the three coloured LED and one for the infrared LED) and a four channel simultaneously updating analogue output module controlled by personal computer. The board has one RGB LED positioned near the camera lens to provide the flicker stimulus. Single-colour-control of the RGB LED allows us to obtain different spectra of the light striking the eye. An IR LED with main emission at 850 nm was used to illuminate the eye under test. Note as, since human vision is not sensitive to this radiation, this illumination does not cause variations in the pupil size. Frequency and magnitude of the flicker was set, for each colour, via personal computer. A target, not shown in Fig. 3, completes the proposed system: the subject under test was asked to spot the target during the measurement thus avoiding pupil size fluctuations due to the pupillary accommodation reflex.

IV. System characterization

Four characterization procedures have been implemented. The first one was aimed at determining the relationship between the parameters of the supply voltage (set by the operator) and the light produced by the LED that strikes the eye. To this purpose, two types of measurements have been carried out aiming at: 1) finding the dominant wavelength of the radiation reaching the eye; 2) getting the relationship between the supply voltage and the optical power emitted by both LEDs. In the second procedure the LEDs (RGB and IR) behaviour over a long period has been verified. Purpose of the third characterization activity is to test the correct performance of the analysis software. Finally, the fourth step is aimed at evaluating the accuracy of the whole pupil size measurement system.

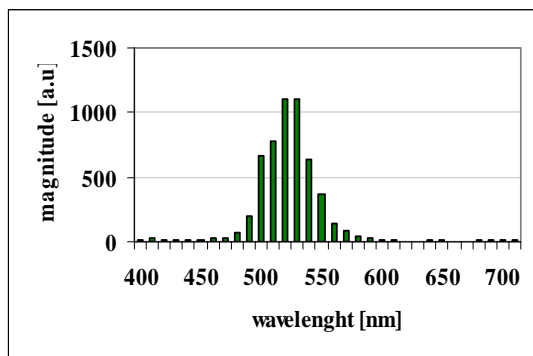


Fig. 4 Spectrum of the light emitted by the green LED

A. Supplying voltage and light

1) Dominant wavelength

The stimulation light is measured by positioning the optical head of a spectrometer sensor instead of the human eye at 10 cm from the light source. The spectrometer (32-channel photosensor module, H8353, Hamamatsu) optical head consists in a mixed fiber bundle (5 mm diameter) that guides the collected light to a multi-cathode photomultiplier tube (PMT). Exploiting a suitable set of interference optical filters, each photocathode is sensitive to a

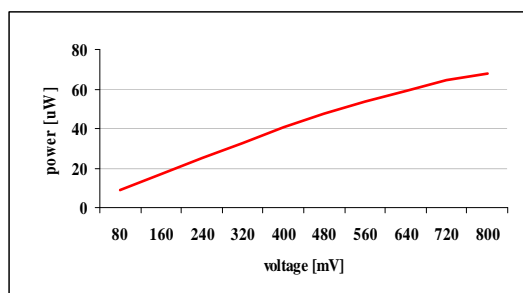


Fig.5 Voltage vs power emitted by red LED

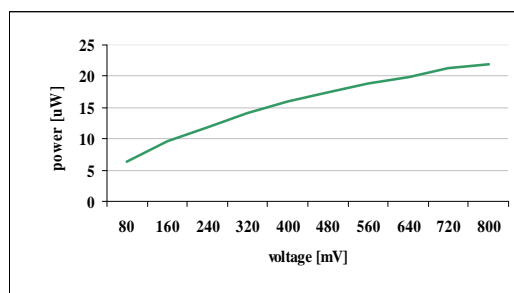


Fig.6 Voltage vs power emitted by green LED

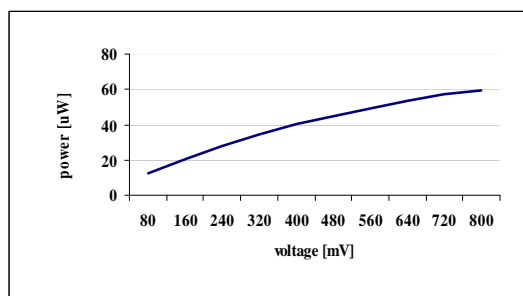


Fig.7 Voltage vs power emitted by blue LED

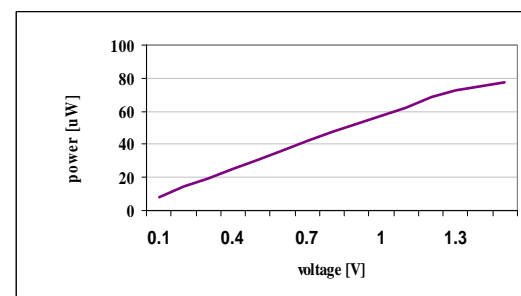


Fig.8 Voltage vs power emitted by IR LED

specific wavelength corresponding to the chromatic channel. The resulting spectral range acquired by the spectrometer is 400 nm - 710 nm with steps of 10 nm. Note as all the chromatic channels are processed simultaneously allowing real time spectral analysis. A sampling frequency of 500 Sa/s (10,000 samples acquired) was set for the spectrometer. The RGB LED has been supplied, one colour at a time, with about 50 mA (the voltage-to-current converter was controlled by 400 mV DC voltage that approximately corresponds to such current). For each colour 20 measurements have been performed. The mean values and standard deviations of each spectral component magnitude have been computed. This way the dominant wavelength of each colour has been determined as one having the highest magnitude: 540 nm for green, 460 nm for blue and 630 nm for red. By way of example, Figure 4 shows the spectrum of the light emitted by the green LED.

2) Optical power emitted by LEDs

The optical power of the light emitted by the RGB and IR LEDs has been measured by a powermeter (Lasercheck Handheld). It features 5%-accuracy in the range 400 nm -1064 nm and can measure powers from 0.5 μ W to 10 mW. The dominant wavelength (detected in the precedent test) has been set and the instrument has been placed at 10 cm from the light source.

As for RGB LED, the supply DC voltage has been varied in the range 80 \div 800 mV with step of 80 mV, whereas DC voltage ranging from 0.1 to 1.5 V with step of 0.1V has been used to supply the IR LED. Ten measurements have been performed and the mean values and standard deviations have been evaluated. Figures 5-6-7-8 report the relationship between the supply voltage and the power irradiated by the red, green, blue and IR component respectively. They show that, as it can be expected, the above relationships are approximately linear, given that the current produced by the converter is proportional to the controlling voltage. Moreover they can be of help in determining the maximum voltage that can be applied without exceeding the maximum permissible exposure (MPE).

In accordance with the IEC 60825 standard [15], the MPE is the highest power or energy density of a light source that is considered safe i.e. that has negligible probability for creating damage. On this base, an MPE equal to 0.001 W/cm² holds for all the considered wavelengths (exposure time 1000 s). By considering a typical pupil diameter of 8 mm, the maximum permissible optical power impinging on the cornea which ensures that the maximum permissible retinal irradiance is not exceeded can be calculated in 500 μ W. Therefore it can be concluded that, for the considered distance from the source, all the used supply voltages can be applied.

B. Performance over a long period of time

A "long run test" of 60 minutes has been performed to verify the behaviour of both the RGB and IR LEDs over a period significantly longer than the usual duration of the measurements on human subject.

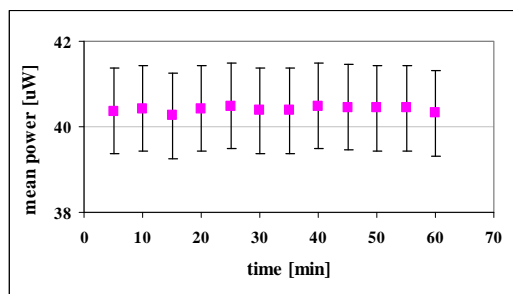


Fig. 9 Mean power emitted by red led measured every 5 min during 1 hour

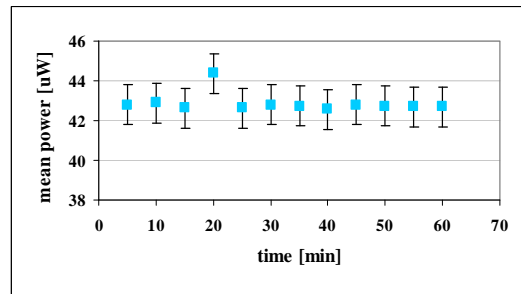


Fig.10 Mean power emitted by IR led measured every 5 min during 1 hour

To this purpose 400 mV and 700 mV DC voltage has been used for supplying RGB and IR LED, respectively, and 5 measurements of the emitted power has been taken every 5 minutes. As usual, mean values and standard deviation has been measured. By way of example the charts in Figure 9-10 report the power emitted by the red and IR LEDs vs. time. The results of the tests on the considered LED have shown that they exhibit a satisfactory behaviour.

C. Test of the analysis software

The correct behaviour of the developed software has been evaluated by processing a set of images (600 x 600 pixels, greyscale bitmap) drawn by using a commercial graphics editing program. Each of them represents a black circle with known diameter and given background colour. Diameter ranging from 108 to 442 pixels has been considered given that they have dimensions similar to the ones of a real human pupil. As for background colours (in 8 bit representation) values of 128, 192 and 255 has been chosen. Figure 11 shows some sample of the test images. The analysis software has provided correct results for the whole set of images. In addition, an image with a white circle simulating an hypothetical reflection in the pupil caused by the IR LED (see the right figure at the second row in Fig. 11) has been used to further test the software. The result, also in this case, has been exact.

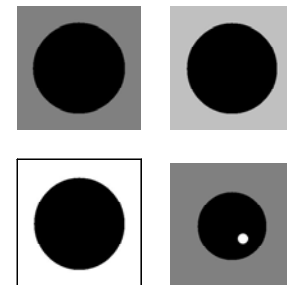


Fig.11 Test images in greyscale bitmap

D. Test of the measurement system

To evaluate the accuracy of the pupil size measurement system, a properly designed set of targets with pictures representing a human eye with different pupil diameters has been used. Diameters from 3 mm to 7 mm with step of 0.5 mm have been considered. Of course, this is a quite simplified representation of the human eye aspect but it can be considered also a very easy way to test the performance of the developed measuring algorithm.

For every camerawork it has been essential to maintain the same conditions: the distance between the lens and the target has been fixed equal to 15 cm; the IR LED has been supplied with 500 mV to have the same environmental light during the acquisitions, and the RGB LED has been supplied with 400 mV. The emitted power has been measured by positioning the powermeter in place of the target at 5 cm from the LEDs; the gauged values have been: 25µW, 31 µW and 15 µW for the red, blue and green light respectively and 3 µW for the IR LED.

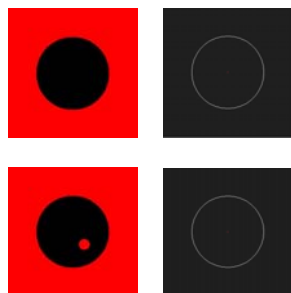


Fig.12 Examples of binarized target images and relevant best fit circle estimated by the software

One hundred pictures have been taken for each pupil diameter and colour (31 fps). The analysis software automatically binaries the acquire image and computes the best circular fitting according to a least square method, thus providing the “pupil” diameter. This way, for each target and illuminating light, the mean values and the standard deviations of the 100 measures are achieved. Fig.12 shows two examples of binary images obtained by processing to acquire image and the relevant best circle. Table 1 reports the mean values and relevant standard deviations of the estimated “pupil” diameter under different test conditions. Two main comments can be drawn. First, as expected, the relationship between the reference and the estimated diameter shows a very good linearity, no matter the incident light. A correlation coefficient equals to 0.999 holds in all the above cases. Moreover, the diameter estimation is slightly dependent on the

Tab.1 Mean values and standard deviations of 100 measurements for each diameter and colour

Reference [mm]	blue		red		green	
	Mean value	Standard deviation	Mean value	Standard deviation	Mean value	Standard deviation
3	198	1	198	0	202	0.2
3.5	234	0	230	0.6	233	1
4	266	0.7	266	0	271	1
4.5	304	0	302	0	306	0.7
5	335	1	334	0	337	1
5.5	366	1	367	1	372	0.2
6	403	0.9	402	0.7	406	0
6.5	438	1	436	0	442	0.2
7	472	0.5	470	0	476	0.7

illuminating colour. In the worst case the maximum difference between corresponding diameters is about 2%. However, it should be underlined that the most important parameter for our purposes is the diameter variation with respect to the one under rest conditions and not the diameter value itself.

V. Conclusions

It is widely recognized that the standard flickermeter must be improved to allow correct measurements in presence of any kind of lamp. However there is a lack of experimental data to validate new model of the complex eye-brain response to flicker. In this light of fact, a pupil size measurement system for the analysis of flicker effect on human being has been presented in this paper. The system allows to both generate flicker with given colour amplitude and frequency and to measure the relevant pupil diameter variation by processing pictures acquired by an high speed high resolution camera. The results of the system characterization have shown its good performance, allowing it to be exploited for collecting useful experimental data.

References

- [1] EN 61000-4-15, "Testing and measurement techniques: flickermeter – functional and design specification," Geneva, Switzerland, 1997.
- [2] IEEE Std. 1453-2004, "IEEE Recommended Practice for Measurement and Limits of Voltage Fluctuations and Associated Light Flicker on AC Power System", New York, USA, 2005.
- [3] EPRI Power Electronics Applications Center, "Lamp Flicker Predicted by Gain-Factor Measurements", Brief n. 36, July 1996
- [4] A. E. Emanuel, L. Peretto, "The response of fluorescent lamp with magnetic ballast to voltage distortion", *IEEE Trans. on Power Delivery*, vol. 12, n. 1, pp.289-294, January 1997.
- [5] D. Gallo, R. Langella, A. Testa, "Light flicker prediction based on voltage spectral analysis", *Proc. of 2001 IEEE Porto Power Tech*, Porto (Portugal), September 2001.
- [6] G. Diez, L.I. Eguiluz, M. Manana, J.C Lavandero, A Ortiz, "Instrumentation and methodology for revision of European flicker threshold", *10th International Conference on Harmonics and Quality of Power*, vol. 1, pp. 262 – 265, 2002
- [7] M. Szlosek, B. Swiętek, Z. Hanzelka, and A. Bien, "Application of neural networks to voltage fluctuations measurement—a proposal for a new flickermeter," *11th International Conference on Harmonics and Quality of Power, 2004*, Lake Placid, USA, September 2004, pp. 403-407.
- [8] A.E. Emanuel, and L. Peretto, "A simple lamp-eye-brain model for flicker observation," *IEEE Trans. on Power Delivery*, vol. 19, n. 3, pp. 1308-1313, 2004.
- [9] L. Peretto, E. Pivello, R. Tinarelli, and A.E. Emanuel, "Theoretical analysis of the physiologic mechanism of luminous variation in eye-brain system," *IEEE Trans. on Instrumentation and Measurement*, vol. 56, n. 1, pp. 164-170, 2007
- [10] L. Peretto, L. Rovati, G. Salvatori, R. Tinarelli, and A.E. Emanuel, "Investigation on the response of the human eye to light flicker produced by different lamps," *IEEE Trans. on Instrumentation and Measurement*, vol. 56, n. 4, pp. 1384-1390, 2007
- [11] D. Gallo, C. Landi, and G. Pasquino, "Design and Calibration of an Objective Flickermeter," *IEEE Trans. on Instrumentation and Measurement*, Vol. 55, n. 6, pp. 2118-2125, 2006.
- [12] Jai, "CM-140 MCL / CB-140 MCL User Manual", Denmark, 2007.
- [13] B. B.Chaudhuri, P. Kundu, "Optimum circular fit to weighted data in multi-dimensional space". *Pattern Recognition Letter*, vol. 14, pp. 1-6, 1993
- [14] Sobel, I., Feldman, G., "A 3x3 Isotropic Gradient Operator for Image Processing", *Pattern Classification and Scene Analysis*, Duda, R. and Hart, P., John Wiley and Sons, '73, pp271-2
- [15] IEC 60825, "Safety of laser products – Part 1: Equipment classification, requirements and user's guide"